A Numerical Study of Scattering From an Object Above a Rough Surface

Joel T. Johnson, *Member, IEEE*

***Abstract*—A numerical model is applied in a Monte Carlo study of scattering from a three-dimensional penetrable object above a lossy dielectric rough interface. The model is based on an iterative method of moments solution for equivalent electric and magnetic surface current densities on the rough interface and equivalent volumetric electric currents in the penetrable object. Both time- and frequency-domain results are investigated to illustrate the relative importance of coherent and incoherent scattering effects in the sample problem considered. Results show that a four-path model using a reduced-reflection coefficient can be reasonable for coherent scattering predictions and that incoherent object/surface interaction effects can make significant contributions to received cross sections.**

***Index Terms*—Electromagnetic scattering, radar cross section, rough surface scattering.**

I. Introduction

ELECTROMAGNETIC scattering from objects is affected by the surrounding medium. Many realistic geometries involve objects in the presence of the Earth surface, which is often modeled as a planar dielectric boundary [1]–[4]. However, roughness on the Earth surface can potentially modify object scattering returns from those with a flat surface, particularly in cases where the roughness size becomes larger than a fraction of the electromagnetic wavelength. Analysis of these problems is complicated by the many possible scattering interactions between the rough surface and object; at present, approximate analytical solutions exist only in the small roughness limit [5]–[9].

Recent works have explored numerical solutions of the combined object/rough surface scattering problem [10]–[13], but have concentrated primarily on two-dimensional (2-D) scattering problems to reduce computational complexity (some three-dimensional (3-D) models have been presented in [14] and [15]). The majority of previous numerical studies have also been directed toward studies of scattering from objects beneath a rough surface for application to ground-penetrating radar problems. Substantial motivation also exists, however, for studying problems in which objects are located above a rough surface, as demonstrated in [13], [16], [17] among other references. Problems of scattering from ships on the sea surface, from airborne objects over terrain, from vegetation above soil surfaces, from automobiles or other vehicles over road or terrain surfaces, all can be classified as combined target/rough surface geometries.

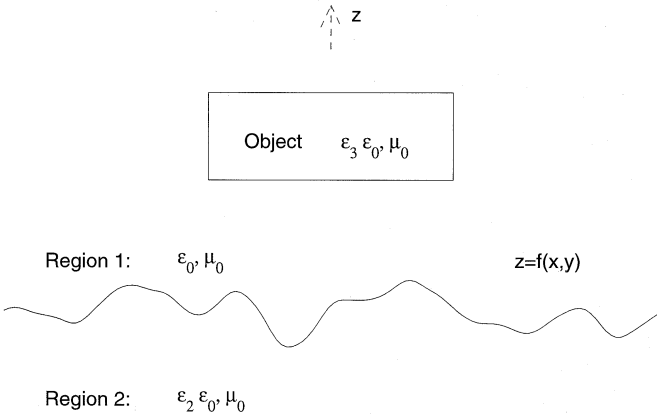

Fig. 1. Geometry of problem.

In this paper, a numerical study of scattering from a 3-D penetrable object located above a lossy dielectric rough interface is performed. Due to the wide range of applications that are addressed by this geometry, a generalized example problem with a relatively low-height object is considered to provide an illustration of some of the coherent and incoherent scattering effects which can occur, and to demonstrate the potential for the method proposed for further studies. A Monte Carlo simulation is used to obtain scattered field statistics as a function of frequency from 2 to 5 GHz and results are illustrated in both the frequency and time domains to clarify the scattering physics. Results show that a "four-path" model [4] can remain reasonable for prediction of total coherent scattered fields if a rough surface reflection coefficient [18] is employed. An examination of incoherent scattered fields shows that object/surface interaction effects can make significant contributions to received cross sections.

The next section briefly reviews the numerical model employed in the study and Section III describes the particular problem for which simulations are performed. Computational issues are discussed in Section IV and results are presented in Section V.

II. Numerical Model

Fig. 1 illustrates the basic geometry considered in this paper: a dielectric object with relative complex permittivity ϵ_3 is located above a rough interface $z = f(x, y)$ (of finite horizontal area as described below) between free space and a dielectric medium

Manuscript received March 2, 2001; revised May 21, 2001. This work was supported in part by the Office of Naval Research under Contract N00014-97-1-0541 and Contract N00014-00-1-0399, by the National Science Foundation under Project ECS-9701678, and by a Grant from Duke University as part of the OSD MURI on Humanitarian Demining. Use of the IBM SP system at the Maui High Performance Computing Center was sponsored by the Air Force Research Laboratory, Air Force Materiel Command under Cooperative Agreement F29601-93-2-0001.

The author is with the Department of Electrical Engineering and Electro-Science Laboratory, The Ohio State University, Columbus, OH 43210 USA (e-mail: johnson@ee.eng.ohio-state.edu).

Digital Object Identifier 10.1109/TAP.2002.802152

with relative complex permittivity ϵ_2. The numerical model applied to solve this problem is an iterative method of moments (MoM) solution for single frequency induced volumetric currents in the dielectric object and induced electric and magnetic surface currents on the rough interface. A point matching formulation is applied and matrix multiply computations required in the iterative method are accelerated through use of the canonical grid method [19], [20] and the discrete dipole approach (DDA) [21], [22] to compute surface to surface and object to object point couplings, respectively, in $O(N \log N)$, where N is the number of surface or object sampling points. A standard iterative method (the "bi-conjugate gradient stabilized" (BiCG-stab) algorithm [23]) is used on the combined object/surface matrix equation and the system is preconditioned through a "flat surface" approximation for surface to surface contributions and a low-accuracy DDA solution for object to object contributions. The model is described in detail in [24], where an example of scattering from an object located below a rough interface is provided. The model is limited by current computing performance to surface geometries which are of moderate size in terms of the electromagnetic wavelength (up to approximately 64λ by 64λ horizontal areas are reasonable at present) and of moderate roughness compared to λ. Target sizes must also remain moderate in terms of the electromagnetic wavelength.

The rough surface profiles used in the study are realizations of a Gaussian random process and for simplicity are chosen to have an isotropic Gaussian correlation function. The resulting surface statistics are described completely by the surface rms height h and correlation length l. Due to the statistical nature of this problem, scattered field results obtained from an ensemble of surface realizations are considered. While a large number of realizations is desirable for more accurate estimates of scattered field statistics, computational issues described in Section IV limit the current study to twenty realizations. Convergence tests with the obtained data show that average cross sections estimates should be accurate to within approximately 3 dB. Both coherent (i.e., cross sections computed from the average field in the Monte Carlo simulation) and incoherent (i.e., cross sections computed from the average power minus the coherent power in the Monte Carlo simulation) are presented. Coherent cross sections provide an estimate of the average scattering behavior while incoherent cross sections provide information regarding the level of variation to be expected for differing rough surface profiles; these statistics can also be used in designing signal processing algorithms for removal of clutter contributions [11]. Although in many applications such averaged results would not be readily available in a given measurement, the coherent and incoherent fields to be presented comprise a basic second-order statistical description of scattering in a combined object/surface problem.

Because the rough interface modeled in the simulation is of finite size, a "tapered wave" incident field is used to avoid surface edge scattering effects. Incidence angles of 0° and 45° from normal incidence are considered in this paper, and the respective tapered wave formulations are provided in [25] and [26]. The tapered waves used in the study are chosen so that the object is well within the 3-dB "spot size" of the incident field while approximately 60-dB incident field attenuation is obtained at surface edges. Tests of tapered wave influence in the flat surface limit have been performed in [4] through comparison with a plane wave incidence halfspace Green's function numerical solution [27]. Results of the comparison show only slight differences (within 1.5 dB) between tapered wave and plane wave radar cross sections obtained from object and object/surface interaction effects. Use of the tapered wave and the finite rough surface horizontal area limit target heights above the surface, which should be limited to approximately the incident field spot radius for the oblique incidence angles considered in the paper. However, since object/surface interactions are of primary interest in this study and since these effects can be more significant for smaller height objects, the results presented should still provide a useful illustration of combined object/surface effects. Methods for addressing target heights beyond these limits are currently being developed.

Due to the presence of both object and distributed source (the rough surface) scatterers, total radar cross sections obtained are dependent on the rough surface area illuminated by the incident tapered wave. For example, in the limit of a very large spot size incident field, rough surface scattering effects become more likely to dominate object scattering effects due to the larger surface area illuminated. To reduce this dependency on the incident field used, scattered fields in the study are calculated both for the combined object/rough surface problem and the rough surface only problem and subtracted to yield "object minus no-object" fields. Coherent and incoherent cross sections obtained from these difference fields then contain only object and object/surface interaction scattering contributions which should be insensitive to the incident field used if the spot size contains the object and regions of the surface which contribute to object/surface interaction effects. Tests with larger tapered wave spot sizes confirmed that difference field cross sections showed only minor variations. Note that the object/surface interaction effects defined here include shadowing of the rough surface by the object as well as other interaction mechanisms. Surface-only incoherent cross sections will also be illustrated and compared with results from the first two terms of the small slope approximation (SSA) [28], but again remain dependent on the area illuminated.

Consideration of the primary scattering effects of this problem suggests that coherent backscattered difference fields should resemble those obtained for an object above a flat surface in the small roughness limit and those obtained for an object in free space in the large roughness limit. A four-path model [4] based on image theory and a single scattering interaction with the object can be developed to describe this process; the basic mechanisms of this model with a flat interface are illustrated in Fig. 2. Evaluating the four-path model requires summing the appropriate object bistatic scattered field for each path with phase shifts according to the path lengths traveled and including Fresnel reflection coefficients for paths that encounter the boundary. To include rough surface coherent scattering effects, the Fresnel reflection coefficients involved in paths two through four are simply multiplied by the standard rough surface reflection coefficient modification [18].

Total incoherent scattered fields should be caused both by direct surface backscattering (not included in the difference

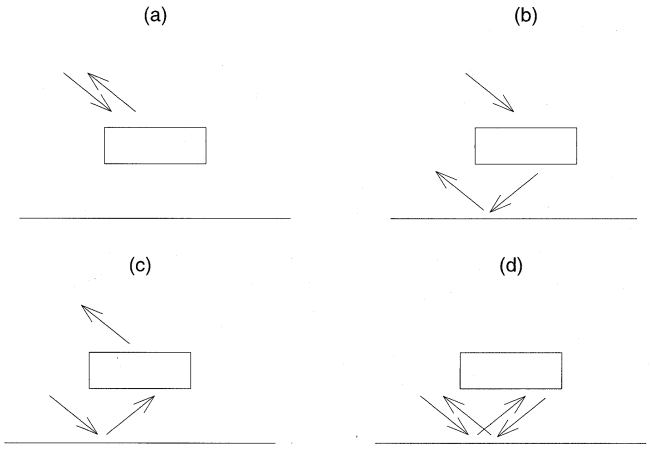

Fig. 2. Scattering mechanisms of four-path model. (a) Path 1. (b) Path 2. (c) Path 3. (d) Path 4.

fields) and by object/surface interaction effects. The four-path model suggests that the latter are likely to be dominated by paths that involve a single bistatic scatter from the object combined with near specular scattering from the rough surface. However, since incoherent scattering from the rough surface is distributed through a range of angles, incoherent object/surface interaction effects can be very complex and difficult to describe completely. Examination of time-domain results in Section V will provide some limited indications as to the most important contributions in the small target height example considered.

III. Example Problem

A dielectric rectangular box with dimensions 7.62 cm by 7.62 cm by 2.54 cm (thickness) and relative permittivity $\epsilon_3 = 3 + i0.03$ is used as the object in this study. The center of the box is located 8.89 cm above the rough interface between free space and a medium with relative permittivity $\epsilon_2 = 5 + i1.25$. Scattering for this geometry is to be determined for a field incident at either 0° or 45° from normal incidence at sixteen frequencies from 2 to 5 GHz. A rough surface correlation length of 3.58 cm and surface rms heights of 3.58 mm or 1 cm are used, so that the surfaces range from slightly rough at the lowest frequency ($kh = 0.15$ or 0.42, respectively, where k is the electromagnetic wavenumber) to slightly to moderately rough at the highest frequency ($kh = 0.375$ or 1.05, respectively). However, rms slopes for these surfaces are approximately 8° and 22°, respectively, making the larger height surface exceed the limitations of standard perturbation theory [29]. The problem considered could model scattering from vegetation components above a soil surface or from a vehicle component above a road surface. Note the problem also scales with frequency, so result implications are not directly limited to the geometrical lengths above.

Time domain scattered fields are obtained from frequency swept data through an FFT operation preceded by multiplication with a third-order Kaiser–Bessel window to reduce sidelobe levels. Time zero is defined to correspond to the center of the mean level of the rough surface ($z = 0$) in Fig. 1, so that object scattering returns occur at negative times. A calculation of expected time delays shows object scattering contributions at approximate times of −0.60 ns and −0.42 ns for 0° and 45° incidence, respectively. Surface-only backscattering returns are centered at time zero and are spread in time from approximately −0.7 ns to 0.7 ns at 45° incidence (calculated from the 3-dB tapered wave spot size.) This time spreading of surface clutter at oblique observation angles and its effects on detection of objects has been previously described in [30]. Time-domain field statistics are calculated in terms of the mean and standard deviation of the field envelope as a function of time to clarify the time locations of various coherent and incoherent scattering effects. Of course, rough surface incoherent scattered fields should show no particular time location, but object/surface incoherent interaction effects do contain some time information that can help to indicate the important scattering mechanisms.

IV. Computational Issues

A 1.281 m by 1.281 m surface size is used which ranges from 8.5 to 21.35 free space wavelengths side dimension as the frequency varies from 2 to 5 GHz. The tapered wave 3-dB spot diameter with parameter $g = 5.333$ [25] is then 28.3 cm so that the object is well within the tapered wave illumination pattern. The interface is sampled into 256 by 256 points, producing a sampling rate of 5.36 points per wavelength in the dielectric medium at the highest frequency; tests with 512 by 512 points in the flat surface limit showed negligible cross section variations. While a smaller number of surface points could be used for the lower frequencies, a constant number of points sampling the rough interface as frequency is varied was chosen for convenience. The resulting number of field unknowns on the interface is 262 144. A "strong" bandwidth of 15 points and one canonical grid series term were used in rough surface matrix elements, as described in [24]; single realization tests confirmed that these parameters should provide accurate results.

The object is sampled on a 32×32×8 point grid with step size 3.175 mm (ranging from approximately 1/27 to 1/11 of the wavelength in the object as frequency varies), resulting in a total number of 13 824 object unknowns. The combined problem thus contains approximately 276 000 unknowns. While this large number of unknowns would be prohibitive for many integral equation based methods, the efficient algorithm applied makes the current study possible.

Although, the problem considered can be solved on a PC level platform for a single realization, total computing times for the multiple cases considered in this paper were further reduced through use of IBM SP parallel computing resources at the Maui High Performance Computing Center [31]. Since results as a function of frequency for multiple realizations were of interest, single frequency-single realization calculations were performed on individual nodes of the parallel computer (comparable to PC platforms) to obtain twenty realizations with 16 frequencies between 2–5 GHz. Single frequency computing times on a single node ranged from approximately six to fourteen hours depending on frequency, incidence angle, and surface statistics; further studies of method parameter choices and alternate iterative algorithms [24] would be likely to allow reduction of these computing times. Four-path model contributions were calculated using an object in free space DDA code [21], [22] with the same grid as in the combined surface/object code and synthesized following the procedure described in [4].

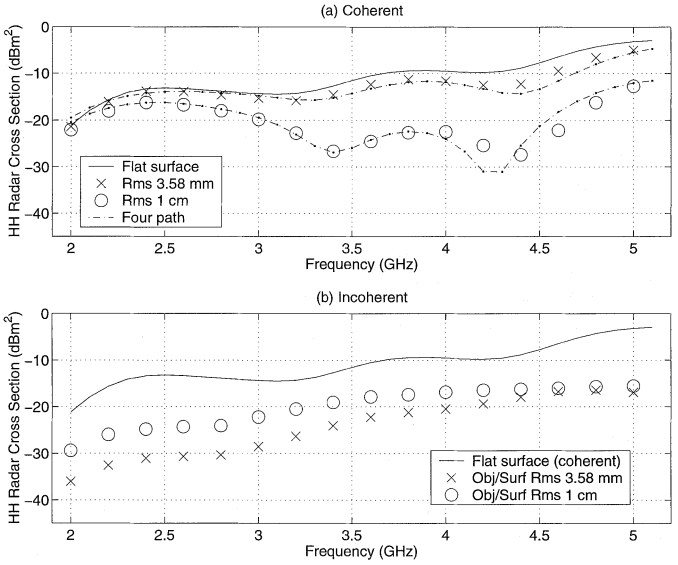

Fig. 3. Average object minus no-object backscattered radar cross sections versus frequency for 0° incidence. (a) Coherent. (b) Incoherent.

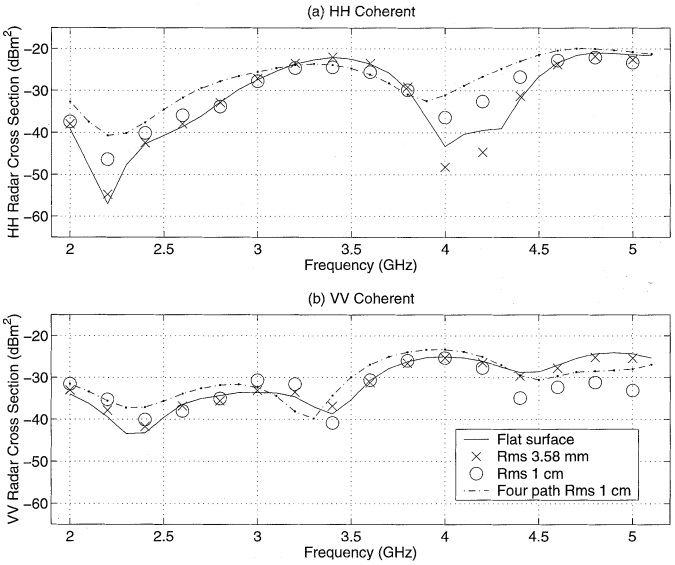

Fig. 4. Coherent object minus no-object backscattered radar cross sections versus frequency for 45° incidence. (a) *HH*. (b) *VV*.

V. Results

A. Frequency Domain

Fig. 3 plots average coherent [plot (a)] and incoherent [plot (b)] object minus no-object backscattered copolarized radar cross sections versus frequency for 0° observation and for both the rms height 3.58 mm and 1 cm cases. Also included are the corresponding cross sections for the object above a flat surface, as well as predictions for coherent cross sections using the reduced reflection coefficient four-path model. Coherent cross sections for the 3.58-mm rms height surface are very similar to those obtained with the object above a flat surface, while those for the rougher surface are significantly different and approach those for the object in free space. The four-path model is found to perform very well for this case, indicating that its approximations remain reasonable even in the presence of rough surfaces. The success of the four-path model indicates that terms involving more than one object scattering process can be neglected for normal incidence in this problem.

Incoherent object/surface interaction cross sections in plot (b) are found generally to increase with frequency, as expected for these surface statistics since more power in coherent fields is converted to incoherent power at higher frequencies. For the smaller rms height surface, total incoherent scattering contributions remain smaller than coherent returns, while incoherent scattering is larger than coherent scattering at some frequencies for the rougher surfaces. The latter case demonstrates that object/rough surface interaction effects can make important contributions to total object scattering so that object returns above differing rough surface profiles can vary significantly.

Figs. 4 and 5 illustrate coherent and incoherent scattering returns, respectively, for 45° incidence in *HH* [plot (a)] and *VV* [plot (b)] polarizations. Polarization differences should be observable in this problem for oblique incidence backscattering due to polarized object scattering and due to the polarization sensitivity of rough surface scattering at oblique angles. Coherent cross sections indeed show significant differences

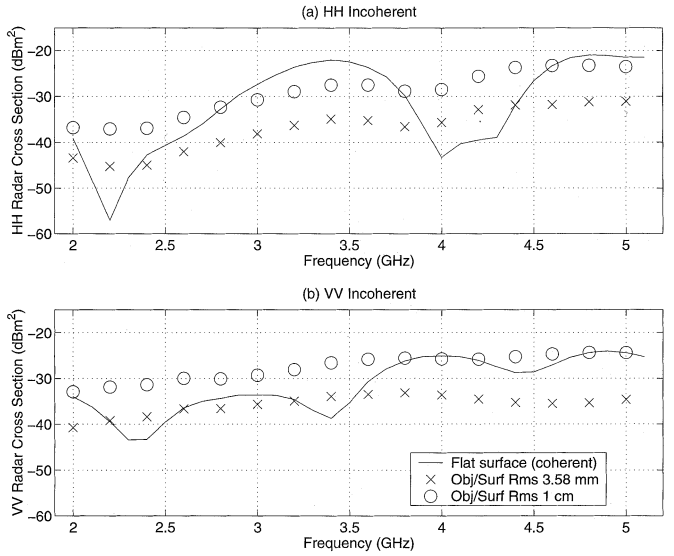

Fig. 5. Incoherent object minus no-object backscattered radar cross sections versus frequency for 45° incidence. (a) *HH*. (b) *VV*.

between *HH* and *VV* returns. Differences of rough surface coherent cross sections from those with a flat surface are less noticeable than in the 0° case, due to the reduced Rayleigh parameters obtained at oblique incidence and smaller differences between the object in free space and object above a flat surface returns at 45°. The accuracy of the four-path model (plotted only for the rougher surface case) is also reduced compared to Fig. 3; similar levels of error are observed when comparing four-path and numerical model results with a flat surface. These discrepancies indicate that paths involving more than one object scattering process are more important for oblique paths, as discussed in [4].

Incoherent returns in Fig. 5 show that incoherent object/surface interactions can be greater than coherent scattering even with the small height surface at some frequencies. Incoherent returns for the larger-height surface are comparable to or greater

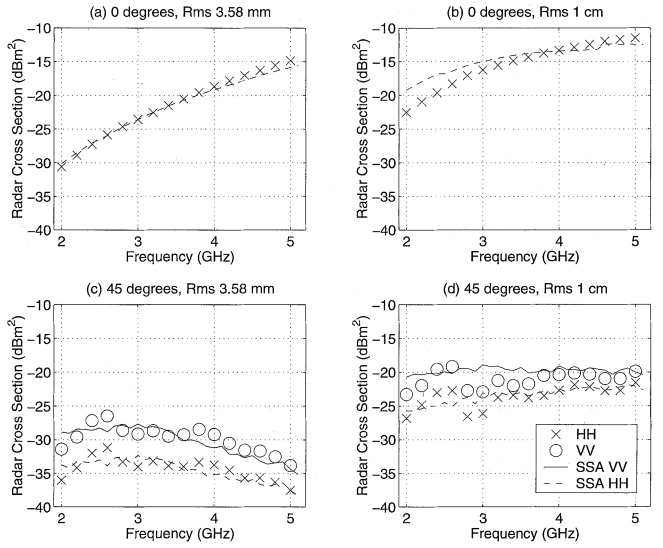

Fig. 6. Comparison of rough surface-only incoherent backscattering with small slope approximation versus frequency. (a) 0° incidence, rms height 3.58 mm. (b) 0° incidence, rms height 1 cm. (c) 45° incidence, rms height 3.58 mm. (d) 45° incidence, rms height 1 cm.

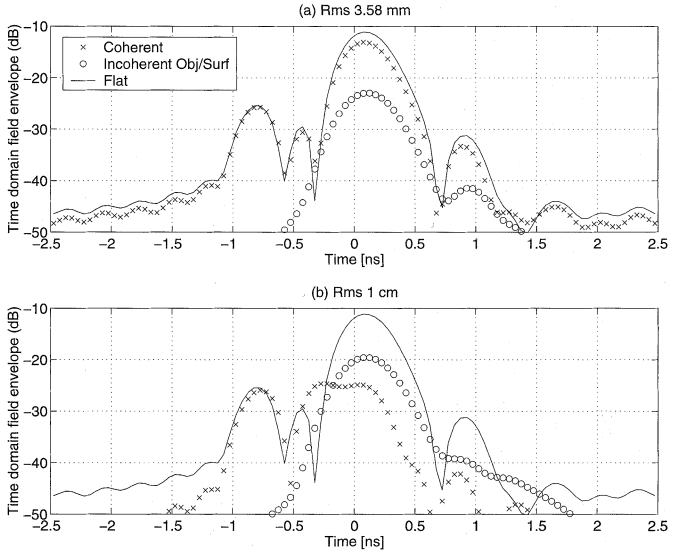

Fig. 7. Envelope of time domain object minus no-object backscattered fields for 0° incidence. (a) Surface rms height 3.58 mm. (b) Surface rms height 1 cm.

than coherent returns at almost all frequencies for both *HH* and *VV* polarizations. A generally increasing trend with frequency in *HH* is again observed, while *VV* results in the low rms height case show a slight decreasing trend at higher frequencies. Explanation of these dependencies is difficult given the many possible scattering interactions between object and surface.

A validation of rough surface-only incoherent cross sections for the specified tapered beam is presented in Fig. 6, where results at 0° [plots (a) and (b)] and 45° [plots (c) and (d)] are compared with predictions of the first two terms of the SSA. A Monte Carlo simulation using 100 surface realizations was used to obtain SSA results [32], so that the curves obtained show some residual variations due to the finite number of realizations. Numerical model results are in good general agreement with the SSA, although some differences within approximately 4 dB at the lower frequencies (where the tapered wave causes a larger degree of angular averaging) are observed. Overall, the reasonable agreement obtained however validates both the numerical model and the SSA prediction for the surfaces considered. Incoherent surface only scattering at 0 degrees generally increases with frequency, while cross sections at 45° show a decreasing trend in the small height case and only slight increases for the rougher surface. Comparisons with object/surface interaction incoherent returns in Figs. 3 and 5 show that surface-only incoherent scattering generally dominates object/surface interaction incoherent effects for the tapered beam used, except at higher frequencies and in *HH* polarization for the smaller height surface.

B. Time Domain

Fig. 7 presents time-domain object minus no-object backscattered field envelopes (in decibels) for 0° incidence in the rms height 3.58 mm [plot (a)] and rms height 1 cm [plot (b)] cases. Both coherent and "incoherent" (i.e., the standard deviation of the field envelope as a function of time) returns are included, as well as returns with the object above a flat surface. Incoherent returns again include object/surface interaction contributions only. Coherent returns in Fig. 7 show general agreement with flat surface results for the lower rms height surface, but appreciable differences for the rougher surface. Note object scattering returns centered around time -0.6 ns show only minor deviations from the flat surface case since no surface scattering sources have been encountered (other than sidelobe contributions from later times.) The large returns appearing around time zero in the flat surface case demonstrate the importance of the bistatic object/surface interaction mechanism of the four-path model for this geometry, because fields scattered from the target into a near specular scattering from the surface or *vice-versa* will still appear around time zero [4]. Coherent returns around time zero in the rms height 1 cm case begin to approach results with the object in free space (not plotted). Incoherent scattering contributions at 0° occur primarily at times after initial object returns, so that time domain object detection strategies would be likely to work well in this case, particularly for the smaller height surface. Initial object/surface incoherent interaction effects are found to be slightly time shifted from time zero, where surface-only scattering would be centered in time. This is consistent with the dominant four-path mechanism of a bistatic scattering from the object followed by a specular scattering from the rough surface, since a transmission through the object would result in a slight time delay. Object/surface interaction effects are also observed to show effects at later times, as would be expected for multiple object/surface interactions.

Figs. 8 and 9 illustrate *HH* [plot (a)] and *VV* [plot (b)] time domain statistics for the rms height 3.58 mm and 1 cm cases, respectively, for 45° incidence. Similar observations regarding coherent fields are obtained in this case, with only slight differences from flat surface returns observed with rms height 3.58 mm, while larger differences are observed in the rougher case as coherent fields approach those for an object in free space. Incoherent returns generally show a greater degree

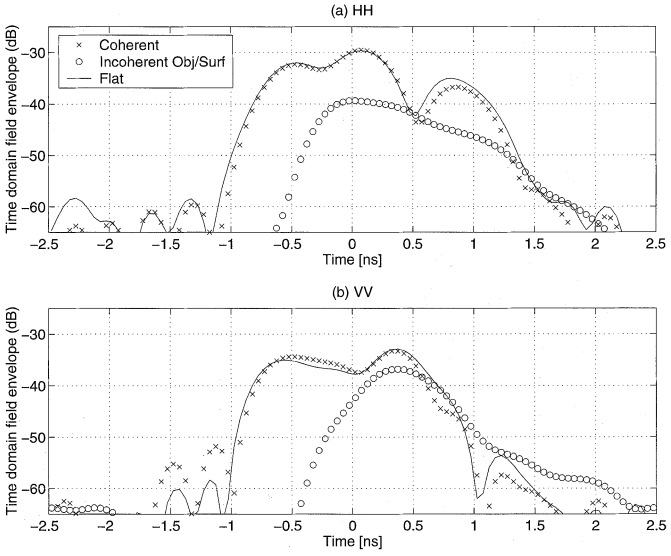

Fig. 8. Envelope of time-domain object minus no-object backscattered fields for 45° incidence: surface rms height 3.58 mm. (a) *HH*. (b) *VV*.

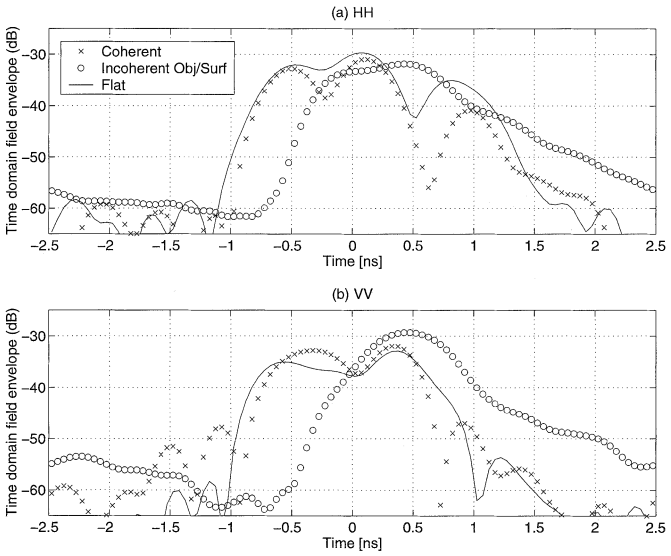

Fig. 9. Envelope of time-domain object minus no-object backscattered fields for 45° incidence: surface rms height 1 cm. (a) *HH*. (b) *VV*.

of time spreading than in Fig. 7, so that less "object-only" time is available before incoherent effects increase, potentially making object detection more difficult. Incoherent scattering is generally comparable to coherent scattering for the rougher surface case, again indicating that a large degree of variation in time domain object returns would be observed as different surface profiles are encountered.

For comparison, time-domain surface-only backscattered field envelopes are plotted in Fig. 10 for 0° [plots (a) and (b)] and for 45° [plots (c) and (d)]. Incoherent returns for these slight to moderately rough surfaces at 0° observation show a time spread that is determined by the 3-GHz bandwidth and envelope function used, while returns at 45° are spread in time according to the tapered wave spot size. The resulting field envelopes at oblique incidence are distributed near-uniformly through the incident field illumination range, although some residual variations due to the finite number of realizations averaged remain. Note, that surface-only returns in the oblique case occur at times prior to the object-only scattering in Figs. 8 and 9, showing again that object detection could be difficult for these geometries. Surface incoherent cross sections for the tapered wave used also are typically larger than object/surface interaction incoherent effects, except at later times in some cases.

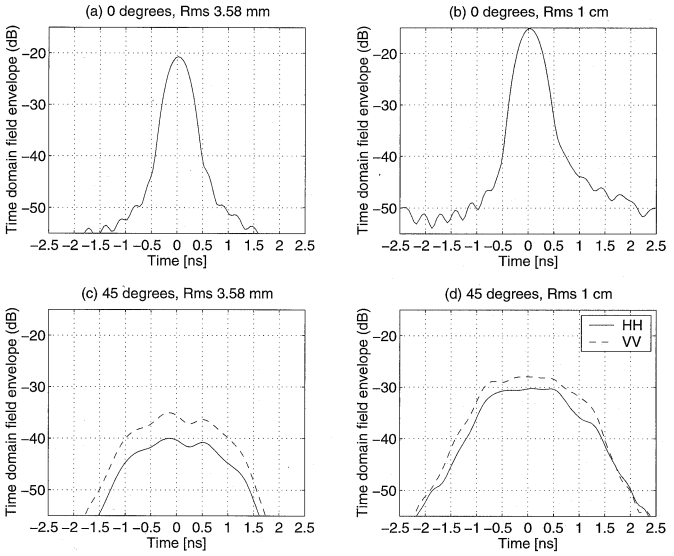

Fig. 10. Envelope of time-domain surface-only incoherent backscattered fields (a) 0° incidence, rms height 3.58 mm. (b) 0° incidence, rms height 1 cm. (c) 45° incidence, rms height 3.58 mm. (d) 45° incidence, rms height 1 cm.

VI. Conclusion

The results of this study demonstrate some of the coherent and incoherent scattering effects that can occur in combined object/rough surface scattering problems. Coherent cross sections were found to resemble those for an object above a flat surface in the small roughness limit but to approach those for an object in free space as the roughness increased. A four-path model using a rough surface reduced reflection coefficient was found to match coherent cross sections well for normal incidence observation, although the accuracy was degraded at oblique observation where multiple object scattering effects can become more important. Incoherent scattered fields in both the time and frequency domains show that both direct surface backscattering and object/surface interaction terms can be important depending on the frequency, surface statistics, polarization, incident antenna pattern, and scattering geometry. Incoherent object/surface interaction effects observed appear consistent with a four-path model interpretation in which the dominant contribution is from an object bistatic scattering followed or preceded by surface forward scattering, although complete conclusions in this regard are difficult to obtain due to the complexity of the object/surface interaction process. Overall results indicate that both rough surface backscattering and bistatic scattering effects should be considered when analyzing returns from an object above a rough surface. Further applications of these results and the iterative method of moments (MoM) model include evaluation of approximate models

for combined surface/object problems [5]–[9], design of improved matched filters for signal processing algorithms, and tests of target detection techniques in the presence of rough surface clutter.

ACKNOWLEDGMENT

The author would like to thank Dr. R. J. Burkholder of the ElectroScience Laboratory for helpful discussions. Opinions, interpretations, conclusions and recommendations are those of the author and are not necessarily endorsed by the United States Air Force, Air Force Research Laboratory, or the U.S. Government.

REFERENCES

[1] J. Q. He, T. J. Yu, N. Geng, and L. Carin, "Method of moments analysis of electromagnetic scattering from a general three-dimensional dielectric target embedded in a multilayered medium," *Radio Sci.*, vol. 32, pp. 305–313, 2000.

[2] N. Geng, M. A. Ressler, and L. Carin, "Wide-band VHF scattering from a trihedral reflector situated above a lossy dispersive halfspace," *IEEE Trans. Geosci. Remote Sensing*, vol. 37, pp. 2609–2617, Sept. 1999.

[3] T. J. Cui and W. C. Chew, "Fast algorithm for electromagnetic scattering by buried 3-D dielectric objects of large size," *IEEE Trans. Geosci. Remote Sensing*, vol. 37, pp. 2597–2608, Sept. 1999.

[4] J. T. Johnson, "A study of the four-path model for scattering from an object above a halfspace," Microwave Opt. Technol. Lett., vol. 30, pp. 130–134, July 2001.

[5] Y. Zhang, Y. E. Yang, H. Braunisch, and J. A. Kong, "Electromagnetic wave interaction of conducting object with rough surface by hybrid SPM/MOM technique," *PIER 22: Progress Electromagn. Res.*, vol. 22, pp. 315–335, 1999.

[6] A. Ishimaru, J. D. Rockway, and Y. Kuga, "Rough surface Green's function based on the first-order modified perturbation and smoothed diagram methods," *Waves Random Media*, vol. 10, pp. 17–31, 2000.

[7] T. Chiu and K. Sarabandi, "Electromagnetic scattering interaction between a dielectric cylinder and a slightly rough surface," *IEEE Trans. Antennas Propagat.*, vol. 47, pp. 902–913, <May 1999.

[8] J. T. Johnson, "Thermal emission from a layered medium bounded by a slightly rough interface," *IEEE Trans. Geosci. Remote Sensing*, vol. 39, pp. 368–378, Feb. 2001.

[9] I. M. Fuks and A. G. Voronovich, "Wave diffraction by rough interfaces in an arbitrary plane-layered medium," *Waves Random Media*, vol. 10, pp. 253–272, 2000.

[10] K. O'Neill, R. F. Lussky, and K. D. Paulsen, "Scattering from a metallic object embedded near the randomly rough surface of a lossy dielectric," *IEEE Trans. Geosci. Remote Sensing*, vol. 34, pp. 367–376, Mar. 1996.

[11] T. Dogaru and L. Carin, "Time-domain sensing of targets buried under a rough air-ground interface," *IEEE Trans. Antennas Propagat.*, vol. 46, pp. 360–372, Mar. 1998.

[12] A. V. der Merwe and I. J. Gupta, "A novel signal processing technique for clutter reduction in GPR measurements of small, shallow land mines," *IEEE Trans. Geosci. Remote Sensing*, vol. 38, pp. 2627–2637, Nov. 2000.

[13] M. R. Pino, L. Landesa, J. Rodriguez, F. Obelleiro, and R. J. Burkholder, "The generalized forward-backward method for analyzing the scattering from targets on ocean-like rough surfaces," *IEEE Trans. Antennas Propagat.*, vol. 47, pp. 961–969, June 1999.

[14] S. Tjuatja, A. K. Fung, and J. Bredow, "Radar imaging of buried objects," in *Proc. IGARSS'98 Conf.*, Seattle, WA, July 1998, pp. 524–526.

[15] G. F. Zhang, L. Tsang, and K. Pak, "Angular correlation function and scattering coefficient of electromagnetic waves scattered by a buried object under a two-dimensional rough surface," *J. Opt. Soc. Amer. A*, vol. 15, pp. 2995–3002, 1998.

[16] M. A. Sletten, D. B. Trizna, and J. P. Hansen, "Ultrawide-band radar observations of multipath propagation over the sea surface," *IEEE Trans. Antennas Propagat.*, vol. 44, pp. 646–651, May 1996.

[17] E. A. Shtager, "An estimation of sea surface influence on radar reflectivity of ships," *IEEE Trans. Antennas Propagat.*, vol. 47, pp. 1623–1627, Oct. 1999.

[18] L. Tsang, J. A. Kong, and R. T. Shin, *Theory of Microwave Remote Sensing*. New York: Wiley, 1985.

[19] L. Tsang, C. H. Chan, K. Pak, and H. Sangani, "Monte Carlo simulations of large scale problems of random rough surface scattering and applications to grazing incidence with the BMIA/canonical grid method," *IEEE Trans. Antennas Propagat.*, vol. 43, pp. 851–859, July 1995.

[20] J. T. Johnson, R. T. Shin, J. A. Kong, L. Tsang, and K. Pak, "A numerical study of the composite surface model for ocean scattering," *IEEE Trans. Geosci. Remote Sensing*, vol. 36, pp. 72–83, Jan. 1998.

[21] B. T. Draine and P. J. Flatau, "Discrete-dipole approximation for scattering calculations," *J, Opt. Soc. Amer. A*, vol. 11, pp. 1491–1499, 1994.

[22] P. J. Flatau, "Improvements in the discrete-dipole approximation method of computing scattering and absorption," *Opt. Lett.*, vol. 22, pp. 1205–1207, 1997.

[23] R. Barrett, M. Berry, T. Chan, J. Demmel, J. Donato, J. Dongarra, V. Eijkhout, R. Pozo, C. Romine, and H. van der Vorst. (1993) Templates for the solution of linear systems: Building blocks for iterative methods. [Online]. Available: ftp netlib2.cs.utk.edu

[24] J. T. Johnson and R. J. Burkholder, "Coupled canonical grid/discrete dipole approach for computing scattering from objects above or below a rough interface," *IEEE Trans. Geosci. Remote Sensing* , vol. 39, pp. 1214–1220, June 2001.

[25] K. Pak, L. Tsang, C. H. Chan, and J. T. Johnson, "Backscattering enhancement of electromagnetic waves from two dimensional perfectly conducting random rough surfaces based on Monte Carlo simulations," *J. Opt. Soc. Amer.*, vol. 12, pp. 2491–2499, 1995.

[26] J. T. Johnson, R. T. Shin, J. A. Kong, L. Tsang, and K. Pak, "A numerical study of ocean polarimetric thermal emission," *IEEE Trans. Geosci. Remote Sensing*, vol. 37, pp. 8–20, Jan. 1999.

[27] E. Newman, "A User's Manual for The Electromagnetic Surface Patch Code: Preliminary Version ESP5.0," ElectroScience Lab., The Ohio State Univ., 1997.

[28] A. G. Voronovich, *Wave Scattering From Rough Surfaces*. Berlin, Germany: Springer-Verlag, 1994.

[29] S. O. Rice, "Reflection of electromagnetic waves from slightly rough surfaces," *Commun. Pure Appl. Math.*, vol. 4, pp. 361–378, 1951.

[30] J. L. Salvati, C. C. Chen, and J. T. Johnson, "Theoretical study of a surface clutter reduction algorithm," in *Proc. IEEE Geosci. Remote Sensing Symp.*, Seattle, WA, 1998, pp. 1460–1462.

[31] (2002) Maui High Performance Computing Center World Wide Web Site. [Online] www.mhpcc.edu.

[32] S. T. McDaniel, "Acoustic and radar scattering from directional seas," *Waves in Random Media*, vol. 9, no. 4, pp. 537–549, 1999.

Joel T. Johnson (M'96) received the B.S. degree in electrical engineering from the Georgia Institute of Technology, Atlanta, in 1991 and the S.M. and Ph.D. degrees from the Massachusetts Institute of Technology, Cambridge, in 1993 and 1996, respectively.

He is currently an Associate Professor in the Department of Electrical Engineering and ElectroScience Laboratory of The Ohio State University, Columbus. His research interests include microwave remote sensing, propagation and electromagnetic wave theory.

Dr. Johnson is a Member of Commissions B and F of the International Union of Radio Science (URSI) and a Member of Tau Beta Pi, Eta Kappa Nu, and Phi Kappa Phi. He received the 1993 Best Paper Award from the IEEE Geoscience and Remote Sensing Society, was named an Office of Naval Research Young Investigator, National Science Foundation Career Awardee, and PECASE Award Recipient in 1997, and was recognized by the U.S. National Committee of URSI as a Booker Fellow in 2002.